BIOCHEMISTRY
including biophysical chemistry & molecular biology

Article

pubs.acs.org/biochemistry

Conformation-Dependent Human p52Shc Phosphorylation by Human c-Src

Yuko Tsutsui,[†] Jennifer M. Johnson,[†] Borries Demeler,[‡] Michael T. Kinter,[§,∥] and Franklin A. Hays*[,†,⊥,▽]

[†]Department of Biochemistry and Molecular Biology, University of Oklahoma Health Sciences Center, Oklahoma City, Oklahoma 73104, United States

[‡]Department of Biochemistry, The University of Texas Health Sciences Center at San Antonio, 7750 Floyd Curl Drive, San Antonio, Texas 78229-3900, United States

[§]Free Radical Biology & Aging Research Program, Oklahoma Medical Research Foundation, Oklahoma City, Oklahoma 73104, United States

[∥]Department of Geriatric Medicine, Reynolds Oklahoma Center on Aging, University of Oklahoma Health Sciences Center, Oklahoma City, Oklahoma 73104, United States

[⊥]Stephenson Cancer Center, University of Oklahoma Health Sciences Center, Oklahoma City, Oklahoma 73104, United States

[▽]Harold Hamm Diabetes Center, University of Oklahoma Health Sciences Center, Oklahoma City, Oklahoma 73104, United States

Supporting Information

ABSTRACT: Phosphorylation of the human p52Shc adaptor protein is a key determinant in modulating signaling complex assembly in response to tyrosine kinase signaling cascade activation. The underlying mechanisms that govern p52Shc phosphorylation status are unknown. In this study, p52Shc phosphorylation by human c-Src was investigated using purified proteins to define mechanisms that affect the p52Shc phosphorylation state. We conducted biophysical characterizations of both human p52Shc and human c-Src in solution as well as membrane-mimetic environments using the acidic lipid phosphatidylinositol 4-phosphate or a novel amphipathic detergent (2,2-dihexylpropane-1,3-bis-β-D-glucopyranoside). We then identified p52Shc phosphorylation sites under various solution conditions, and the amount of phosphorylation at each identified site was quantified using mass spectrometry. These data demonstrate that the p52Shc phosphorylation level is altered by the solution environment without affecting the fraction of active c-Src. Mass spectrometry analysis of phosphorylated p52Shc implies functional linkage among phosphorylation sites. This linkage may drive preferential coupling to protein binding partners during signaling complex formation, such as during initial binding interactions with the Grb2 adaptor protein leading to activation of the Ras/MAPK signaling cascade. Remarkably, tyrosine residues involved in Grb2 binding were heavily phosphorylated in a membrane-mimetic environment. The increased phosphorylation level in Grb2 binding residues was also correlated with a decrease in the thermal stability of purified human p52Shc. A schematic for the phosphorylation-dependent interaction between p52Shc and Grb2 is proposed. The results of this study suggest another possible therapeutic strategy for altering protein phosphorylation to regulate signaling cascade activation.

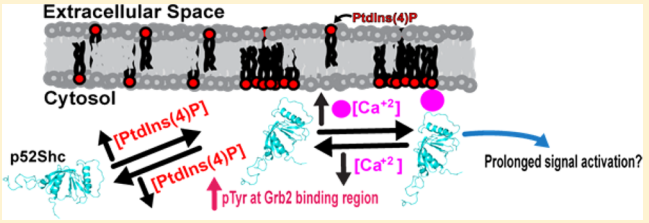

Adaptor proteins facilitate the assembly of protein complexes that modulate signaling cascade activity.[1] Protein phosphorylation plays a central role in the spatiotemporal activation of these signaling cascades by determining the order, and affinity, of signaling complex assembly in response to receptor activation.[2] Aberrant signaling pathway activation is associated with the pathogenesis of human disease, including cancer and diabetes,[3,4] so understanding adaptor protein phosphorylation is a fundamental component of linking pathway activation to disease onset and progression. A predominant player in signaling complex assembly is the p52Shc adaptor protein that regulates a wide array of cellular processes, including insulin and lipid signaling, endocytosis, ubiquitination, and the Ras/MAPK/ERK pathways.[5,6] Indeed, the breadth of protein−protein interactions for p52Shc is demonstrated by a recent mass spectrometry study that identified the murine p52Shc phosphorylation interactome, comprised of 41 different binding partners, in response to EGF-dependent signal activation.[6] These protein−protein interactions are facilitated by the modular domain architecture of p52Shc, which consists of N-terminal phosphotyrosine binding (PTB), central collagen homology-1 (CH1), and C-terminal Src homology-2 (SH2) domains,[5,7] each of which contains known and putative phosphorylation sites.

One of the most heavily studied p52Shc binding interactions, using both *in vivo* and *in vitro* systems, is that with the Grb2

Received: February 6, 2015
Revised: April 30, 2015
Published: May 11, 2015

DOI: 10.1021/acs.biochem.5b00122
Biochemistry 2015, 54, 3469−3482

adaptor protein.[5,6,8−10] In v-Src-transformed Rat-2 cells, tyrosine phosphorylation at residues 239, 240, and 318 in the CH1 domain of p52Shc recruits Grb2, leading to activation of the Ras/MAPK signaling pathway.[7,8] Using HA-tagged p52Shc isolated from EGF-stimulated and v-Src-transfected COS1 cells, it was shown that doubly phosphorylated p52Shc at Tyr239/240 bound to the SH2 domain of Grb2 more strongly than singly phosphorylated p52Shc at Tyr318,[9] suggesting that the enhanced interaction between p52Shc and Grb2 may underlie aberrant prolonged activation of the various signaling cascades, resulting in pathological conditions. If this is so, defining a molecular mechanism for p52Shc site-specific tyrosine phosphorylation could be beneficial for developing novel therapeutic interventions to potentiate signaling cascade activity. Indeed, this idea is supported by the observation that bovine c-Src phosphorylates a GST-p52Shc fusion protein at Tyr239 or Tyr240 only in the presence of the acidic lipid phosphatidylinositol 4-phosphate [PtdIns(4)P],[11] suggesting that the p52Shc conformation and local environment are driving factors in determining the phosphorylation state. How this local environment may drive signaling complex formation, whether it is formed in the cytoplasm followed by migration to the activated receptor or formed directly on the membrane surface, is not known. The current model suggests p52Shc is phosphorylated in the cytoplasm that, in turn, leads to binding partner (e.g., Grb2) assembly and migration of the bound complex to the membrane surface where it interacts with the receptor tyrosine kinase.[5]

In this study, we examined c-Src-mediated phosphorylation of p52Shc in aqueous and membrane-mimetic environments using purified proteins. We demonstrate that p52Shc phosphorylation by purified human c-Src is sensitive to solution conditions and suggest how altered phosphorylation may relate to signaling complex formation. Human p52Shc forms specific, and nonspecific, binding interactions with PtdIns(4)P that are mediated by divalent and monovalent cation concentration and pH. Unlike a previous PtdIns(4)P binding study using an isolated PTB domain,[12] the specific PtdIns(4)P binding interaction was observed only in the presence of $CaCl_2$ with full-length human p52Shc. Furthermore, lipid binding led to a decrease in p52Shc thermal stability and altered phosphorylation levels that were independent of c-Src activity and concentration. Addition of a neopentyl glycol detergent [2,2-dihexylpropane-1,3-bis-β-D-glucopyranoside (OGNG)] to purified p52Shc resulted in additional destabilization and altered phosphorylation status. Intriguingly, the p52shc phosphorylation pattern in OGNG showed the same phosphorylation pattern that v-Src did, without affecting the fraction of active c-Src. On the basis of the findings in this study, we propose a model in which p52Shc cellular localization impacts its phosphorylation, its interaction with binding partners, and subsequent activation of downstream signaling cascades.

EXPERIMENTAL PROCEDURES

Cloning, Expression, and Purification of Human p52Shc. A plasmid carrying isoform 7 (307P → PA) of human p52Shc cDNA was obtained from ORIGENE (Rockville, MD). The cDNA fragment was amplified and ligated into a modified pLgals1 plasmid[13] with a C-terminal 3C protease recognition sequence, human galectin-1, and 10-His tag. The DNA sequence of the ligated human p52Shc, encoding residue 1−474, was confirmed by DNA sequencing. The pLgals1-p52Shc plasmid was used to transform Rosetta(DE3) *Escherichia coli* cells (EMD Millipore) with expression of the fusion protein in Luria broth induced by addition of 1 mM isopropyl β-D-thiogalactopyranoside (IPTG). Following induction, cells were grown for 4 h at 30 °C and harvested by a 20 min low-speed spin at 3000*g*. Pelleted cells were resuspended in 20 mM Tris at pH 7.8 at room temperature (pH 7.8RT) (all Tris pH values were measured at room temperature), 1 M NaCl, 25 mM imidazole, and 5% (v/v) glycerol (buffer A) containing 1 mM phenylmethanesulfonyl fluoride (PMSF) at 4 °C. Cells were lysed via sonication (Sonics Vibra Cell VCX500 with 13 mm probe 630-0220) at 50% amplitude (30 s on, 30 min off; 10 cycles) on ice. The total cell lysate was centrifuged at 26000*g* and loaded onto cobalt resin by gravity flow. The resin was washed with 150 mL of buffer A followed by elution using buffer A containing 200 mM imidazole. The elution sample was mixed with His-MBP-3C protease and digested overnight at 4 °C to remove the galectin-1 expression tag while dialyzing against 20 mM Tris pH 7.8RT, 20 mM NaCl, 5 mM β-marcaptoethanol (βME), and 5% (v/v) glycerol. 3C protease was removed using an amylose affinity column with the flow-through collected for subsequent purification. The flow-through was injected onto a 5 mL Hitrap anion exchange Q-column (GE Healthcare) equilibrated in 20 mM Tris pH 7.4RT, 20 mM NaCl, 5% (v/v) glycerol, and 5 mM βME (buffer B) and eluted with buffer B containing 250 mM NaCl. p52Shc fractions were pooled with a final protein concentration determined by the 280 nm absorbance (molar extinction coefficient of 36900 M^{-1} cm^{-1}). Purified p52Shc was stored at 4 °C until it was used. All chemicals were obtained from Sigma or Research Products International unless otherwise specified.

Cloning, Expression, and Purification of Human c-Src. Plasmids carrying human c-Src cDNA[14] or *Yersinia pestis* YopH[15] were purchased from the DNASU Plasmid Repository (https://dnasu.org). The c-Src cDNA segment, encoding residues 86−536, was amplified via polymerase chain reaction and ligated into MCS1 of the CDFDuet-1 plasmid (Novagen) using *Bam*HI and *Hin*dIII restriction sites. To prevent c-Src degradation during *E. coli* expression, we cloned the *Y. pestis* YopH c-DNA sequence into MCS2 of the same plasmid creating a co-expression system with human c-Src as described previously.[16] Plasmid ORF sequences were confirmed by standard DNA sequencing. The CDFDuet1-cSrc-YopH co-expression plasmid was transformed into Rosetta(DE3) (EMD Millipore) *E. coli* cells. Cells were cultured at 37 °C until the OD_{600} reached ≈0.6, at which point the culture temperature was lowered to 30 °C. When the OD_{600} reached 0.9−1.0, cells were induced using 1 mM IPTG and then grown for an additional 4 h at 30 °C prior to cells being harvested via a low-speed spin for 20 min at 3000*g*. A purification protocol for the bacterially expressed kinase domain of c-Src has been described previously,[16] though we observed that modifications were required to purify full-length c-Src containing the SH3, SH2, and kinase domains in the current system. Instead of dialyzing against Tris pH 7.5RT buffer without NaCl, we dialyzed cobalt-eluted c-Src and YopH fractions against 20 mM Tris pH 7.5RT, 20 mM NaCl, 5% (v/v) glycerol, and 1 mM DTT followed by anion exchange purification on a HiTrap Q-column (GE Healthcare). YopH elutes in the flow-through, while c-Src binds to the resin and elutes in 100−150 mM NaCl. c-Src-containing fractions were pooled and concentrated for subsequent size exclusion chromatography (SEC) in 20 mM HEPES (pH 7.4),

DOI: 10.1021/acs.biochem.5b00122
Biochemistry 2015, 54, 3469−3482

Table 1. Genetic Algorithm−Monte Carlo and SV Results from the AUC Experiment[a]

species	molar mass (kDa, measured)	molar mass (kDa, theoretical)	s ($\times 10^{-13}$ s)	f/f_0	amount	R_H (Å)
monomer	63.56 (32.07, 95.06)	63.77	2.96 (2.23, 3.70)	1.95 (1.80, 2.11)	47.1%	52

[a]Values in parentheses are 95% confidence intervals for the respective parameter.

100 mM NaCl, 5% (v/v) glycerol, and 1 mM DTT. The c-Src concentration was determined by the 280 nm absorption (molar extinction coefficient of 83770 M^{-1} cm^{-1}). Thus, a novel bacterial expression and purification system for human c-Src (residues 86−536) containing the SH3, SH2, and kinase domains has been developed. The purified c-Src activity was probed by conducting kinase reactions in 5 mM ATP and 5 mM $MgCl_2$. The presence of activating Tyr419 and the absence of inactive Tyr530 phosphorylation were confirmed by Western blots using the c-Src-specific anti-phospho-Tyr419 or anti-phospho-Tyr530 antibody (catalog no. 6943S or 2105P, respectively, from Cell Signaling Technology).

Circular Dichroism (CD) Spectroscopy. The pooled HiTrap Q-column fractions were dialyzed against 20 mM MOPS (pH 7.4), 100 mM NaCl, and 5% (v/v) glycerol for CD spectroscopy analysis; 100 μM $CaCl_2$ and 30 μM PtdIns(4)P were added to the protein samples following dialysis and prior to CD data collection. CD spectra were recorded using a JASCO J-715 spectropolarimeter equipped with a PTC-348WI temperature controller. Purified p52Shc in a sealed 0.1 cm path-length cuvette was used for measurements with a scan rate of 10 nm/min from 190 to 260 nm. Each sample was scanned three times, and the average of three scans was used for data analysis. Similarly, thermal unfolding of p52Shc was conducted while the CD signal at 207 or 222 nm was being monitored with a rate of heating of 2 °C/min from 25 to 80 °C.

Fluorescence Spectroscopy. The intrinsic tryptophan fluorescence of purified human p52Shc or c-Src at 0.3 or 0.1 μM, respectively, was measured using an ISS photon counting spectrofluorometer in 20 mM MES (pH 5.0) or 20 mM HEPES (pH 7.4) containing 100 mM NaCl and 5% (v/v) glycerol. The excitation wavelength was set at 295 nm, and the emission spectra between 310 and 420 nm were recorded at 25 °C. Each sample was scanned three times, and the average of three scans was analyzed. PtdIns(4)P (Avanti Polar Lipids, Inc.) was dissolved in water to prepare a 1 mM stock. Each sample was equilibrated for 30 min at room temperature prior to data collection. Binding data were fitted using a Langmuir isotherm 1:1 binding model.

Dynamic Light Scattering (DLS). PtdIns(4)P at 30 μM in Tris pH 7.4RT, 100 mM NaCl, and 5% (v/v) glycerol was used for all dynamic light scattering experiments. The data were collected on a Zetasizer Nano Z (Malvern Instruments Ltd.), and the sample scattering intensity was measured three times. The data were averaged to determine the hydrodynamic radii of the PtdIns(4)P cluster.

Analytical Ultracentrifugation (AUC). The p52Shc oligomerization state and conformation were evaluated at a protein loading concentration of 8.7 μM using AUC. The experiments were performed in a Beckman Optima XL-I analytical ultracentrifuge at the Center for Analytical Ultracentrifugation of Macromolecular Assemblies at the University of Texas Health Science Center at San Antonio. Sedimentation velocity experiments were performed at 40000 rpm and scanned at 280 nm in intensity mode, in 20 mM Tris pH 7.4RT and 100 mM NaCl. Experimental data were collected at 20 °C using 1.2 cm Epon two-channel centerpieces (Beckman Coulter). Hydrodynamic corrections for buffer density and viscosity were estimated by UltraScan to be 1.0029 g/mL and 1.0129 cP, respectively. The partial specific volume of p52Shc (0.7276 mL/g) was estimated by UltraScan from protein sequence using a method analogous to the methods outlined in ref 17. All data were analyzed with UltraScan-III version 2.2, release 1743, as previously described.[18] Optimization was performed by two-dimensional spectral analysis (2DSA)[19] with simultaneous removal of time-invariant and radially invariant noise contributions. 2DSA solutions were subjected to parsimonious regularization by genetic algorithm analysis[20] and further refined using Monte Carlo analysis to determine confidence limits for the determined parameters (Table 1).[21] Diffusion-corrected integral sedimentation coefficient distributions were obtained from the enhanced van Holde−Weischet analysis.[22] The calculations were computationally intensive and conducted on high-performance computing platforms.[21] All calculations were performed on the Lonestar cluster at the Texas Advanced Computing Center at the University of Texas at Austin.

Interaction between p52Shc and c-Src Studied by SEC. Equimolar amounts of p52Shc and c-Src (200 μg each) in a total volume of 500 μL were injected onto a Superdex 200 10/300 GL column (GE Healthcare) equilibrated and run in 20 mM HEPES (pH 7.4), 100 mM NaCl, 5% (v/v) glycerol, and 1 mM DTT at a flow rate of 0.5 mL/min on a Hitachi Chromaster liquid chromatography system. Both proteins were incubated and equilibrated for 30 min at 25 °C before SEC injection.

Assessment of p52Shc and c-Src *in Vitro* Phosphorylation. The total protein concentration of each SEC fraction was determined via a BCA assay (Thermo Scientific), and 0.5 μg of total protein (c-Src and p52Shc) was used for kinase reactions in 20 mM HEPES (pH 7.4), 100 mM NaCl, 5 mM $MgCl_2$, and 5 mM ATP at 25 °C for 30 min in a total volume of 20 μL. The reaction was terminated by addition of sodium dodecyl sulfate−polyacrylamide gel electrophoresis (SDS−PAGE) sample buffer, and the samples were run on an 8% (w/v) SDS−PAGE gel and evaluated by Western blotting. After being transferred, polyvinylidene difluoride membranes were blocked with TBST buffer containing 5% (w/v) dry milk. The membranes were incubated in a TBST milk solution containing the anti-phosphotyrosine antibody (catalog no. 8954S from Cell Signaling Technology). The protein was visualized using the HRP-conjugated secondary rabbit anti-IgG antibody (Cell Signaling Technology) followed by addition of chemiluminescent substrate (Thermo Scientific).

Isothermal Titration Calorimetry (ITC). Purified p52Shc was concentrated using 30 kDa molecular mass cutoff Microcon ultracentrifugal filters (EMD Millipore) and then buffer exchanged into 20 mM MOPS (pH 7.4), 100 mM NaCl, and 5% (v/v) glycerol using Econo-Pac 10DG desalting columns. The sample was further dialyzed against the desalting column buffer with three changes of the dialysate, and the dialysate was used to dissolve $CaCl_2$ to prepare the 300 μM titrant. Dialyzed p52Shc at 14 μM was titrated with 5 μL of the $CaCl_2$ stock at each injection at 30 °C, and the data were collected using a VP-

DOI: 10.1021/acs.biochem.5b00122
Biochemistry 2015, 54, 3469−3482

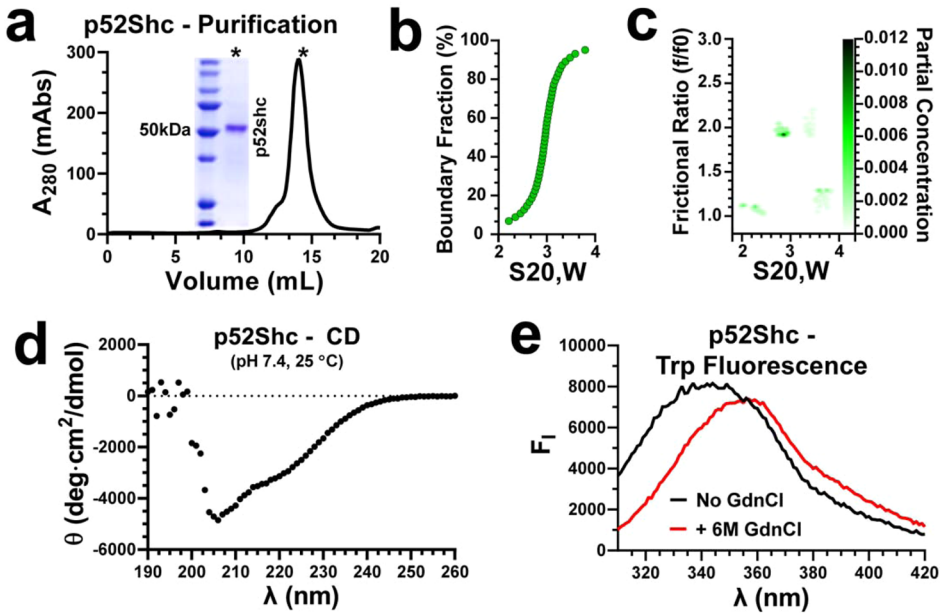

Figure 1. Biophysical properties of human p52Shc. (a) Size exclusion chromatogram of purified full-length human p52Shc (52 kDa). The purified protein was run on a size exclusion column at pH 7.4. The peak fraction corresponding to monomeric p52Shc is shown with an asterisk on the SDS−PAGE gel (inset; left lane, molecular mass marker with the position of 50 kDa indicated) and in the chromatogram. (b) van Holde−Weischet diffusion-corrected sedimentation coefficient distributions for p52Shc determined by AUC with abscissa values corresponding to the sedimentation coefficient corrected for 20 °C and water ("S20,W") and the ordinate corresponding to the percent of the sedimentation boundary with a corresponding *S* value (colored green). (c) Genetic algorithm−Monte Carlo analysis of the AUC data identifying one major species sedimenting around 3 S. Most minor contributions are lower-molecular mass contributions, which suggests that the protein is not involved in mass action. The color gradient indicates partial concentration with the most concentrated species around ∼3 S with a frictional ratio of ∼1.9. (d) Far-UV CD spectrum of purified p52Shc at pH 7.4 and 25 °C. (E) Tryptophan fluorescence spectra of purified p52shc at pH 7.4 in the native state (black line) or in the unfolded state in 6 M guanidine hydrochloride (GdnCl, red line). The excitation wavelength (λ_{ex}) was set to 295 nm.

ITC (Microcal Inc.) instrument. Analysis of ITC data was performed using Origin (OriginLab).

Mass Spectrometry. Kinase reactions were conducted in 20 mM HEPES (pH 7.4), 100 mM NaCl, 5% (v/v) glycerol, and 1 mM DTT using 1 or 0.5 μg of c-Src and 25 μg of p52Shc at 25 °C for 16 h. The reaction samples were loaded onto 10% (w/v) SDS−PAGE gels with protein bands cut from the gel and processed by a standard in-gel digestion. Briefly, the cut bands were washed and destained, reduced with DTT, and alkylated with iodoacetamide. After these reagents had been washed off the gel pieces, the proteins were digested with trypsin at 25 °C overnight. Peptides were gel extracted, evaporated to dryness, and reconstituted in 50 μL of 1% (v/v) acetic acid for analysis. The samples were analyzed using a Thermo Scientific LTQ-XL system with an Eksigent splitless nanoflow high-performance liquid chromatography system. Samples (10 μL) were injected onto a 10 cm × 75 μm capillary reverse phase C18 column (Phenomenex Jupiter). The column was eluted with a 60 min linear gradient of acetonitrile in water with 0.1% (v/v) formic acid (from 3 to 63%). A data-dependent analysis was used to acquire one mass spectrum and nine CID spectra per cycle. Approximately 12000 CID spectra were acquired in each analysis. All spectra were used to search the human RefSeq database with search parameters, including variable modification of serine, threonine, and tyrosine by phosphorylation. Serine and threonine phosphorylation sites were also searched by plotting neutral loss chromatograms for the loss of H_3PO_4. The CID spectra of all phosphorylated peptides were verified by manual interpretation of the spectra. This process was aided by the CID spectra of the corresponding unphosphorylated peptides. Relative phosphopeptide amounts were measured using the Native Reference Peptide method.[23,24] Briefly, the LTQ mass spectrometer was used in the selected reaction monitoring mode to monitor the respective phosphorylated and unphosphorylated versions of each peptide. The relative degree of phosphorylation was then determined by changes in the ratio of the phosphorylated to unphosphorylated peptide.

RESULTS

Full-Length Human p52Shc Adopts a Folded and Extended Conformation in Solution. Full-length human p52Shc (residues 1−474) was expressed as a C-terminal human galectin-10-His fusion protein in *E. coli*. The affinity tag was removed following 3C protease digestion, and p52Shc was purified to homogeneity as judged by SDS−PAGE (Figure 1a, inset). Purified p52Shc is monodisperse in solution at pH 7.4 as demonstrated by SEC (Figure 1a). To further characterize the oligomerization and conformational state of p52Shc in solution, we performed AUC SV experiments. *s* value distributions are shown in the van Holde−Weischet integral distribution plot (Figure 1b), and frictional ratios were determined by Genetic Algorithm−Monte Carlo analysis (Figure 1c). The *s* values, hydrodynamic parameters, and molar masses calculated from the SV experiments are listed in Table 1. The molecular mass found for the predominant species was in excellent agreement with the theoretical molecular mass expected for the monomeric species, while the frictional ratio of p52Shc (1.95) suggests that it is considerably anisotropic, adopting either an unfolded or extended structure. The measured average hydrodynamic radius (R_H) of p52Shc (52 Å) is comparable to the calculated radius of gyration (R_G) for an

DOI: 10.1021/acs.biochem.5b00122
Biochemistry 2015, 54, 3469−3482

extended random coil (72 Å), assuming the power law relationship between chain length and R_G.[25] The average R_H of p52Shc is larger than the R_H of a protein with similar residue length in the globular state, such as the 494-residue yeast triosephosphate isomerase (R_H = 29.7 Å),[26] yet far-UV CD spectra, with two minima at 222 and 207 nm, indicate strong secondary structural elements in purified p52Shc at pH 7.4 (Figure 1d). Furthermore, in the presence of 6 M guanidine hydrochloride, tryptophan fluorescence was red-shifted compared to that of the native tryptophan fluorescence (Figure 1e), indicating that the environment around the tryptophan residues is shielded from the aqueous environment in the native state p52Shc structure. These observations demonstrate that purified p52Shc adopts a folded and extended conformation in solution. This intrinsic flexibility could play an important role in spatiotemporal coordination of interactions between p52Shc and its numerous binding partners identified in a previous study.[6] Scaffolding proteins that recognize multiple binding partners are known to be highly disordered and conformationally variable.[27]

Interaction between Purified p52Shc and PtdIns(4)P Is Modulated by $CaCl_2$ at pH 7.4. A previous centrifugation study showed that among a variety of phospholipids, PtdIns(4)P-containing BrPC vesicles bound most tightly to the isolated N-terminal PTB domain of p52Shc with a K_D of 52 μM at pH 7.4.[12] In the PTB domain, there are two tryptophan residues that can serve as sensitive probes to monitor PtdIns(4)P binding by fluorescence spectroscopy. Because p52Shc is known to function at neutral pH of the plasma membrane surface as well as at acidic pH of endosomal/lysosomal compartments,[28] we tested binding of PtdIns(4)P to the purified full-length p52Shc at both neutral and acidic pH. At pH 5.0 and 7.4 in the absence of p52Shc, PtdIns(4)P formed 91−122 nm clusters (Figure S1 of the Supporting Information), the size comparable to that of PtdIns(4,5)P clusters (80−130 nm) reported previously *in vitro* and *in vivo*.[29−32] At pH 5.0, PtdIns(4)P titration to p52Shc caused quenching of tryptophan fluorescence in a concentration-dependent manner (apparent K_D = 4.1 μM) (Figure 2a). In contrast, although addition of PtdIns(4)P resulted in a decrease in tryptophan fluorescence, no saturable PtdIns(4)P binding was observed at pH 7.4 (data not shown). However, CD spectroscopy indicates changes in p52Shc stability as the presence of PtdIns(4)P lowered the midpoint of thermal unfolding (T_m) by 2 °C (Figure 2b, green line) relative to that of p52Shc alone (Figure 2b, black line). When p52Shc and PtdIns(4)P were incubated at pH 7.4 and analyzed by SEC, p52Shc eluted as a stable higher-molecular mass species (Figure 2c, red line) that was diminished upon addition of 250 mM NaCl (Figure 2c, blue line), indicating that the interaction between p52Shc and PtdIns(4)P at pH 7.4 is reversible and involves weak electrostatic interaction.

Because p52Shc was shown to be involved in lipid signaling,[6] PtdIns(4)P binding was also tested in the presence of calcium, the major modulator of lipid signaling cascades.[33] At pH 7.4 in the presence of 100 μM $CaCl_2$, the tryptophan fluorescence decreased in a PtdIns(4)P concentration-dependent manner as observed at pH 5.0 (Figure 2d). When EDTA was added to a sample containing 200 μM PtdIns(4)P and 100 μM $CaCl_2$, the native state tryptophan fluorescence was recovered (Figure 2d, orange line). Fitting the binding data, while taking nonspecific interactions into account, yielded an apparent K_D value of 9.8 μM in the presence of $CaCl_2$ at pH 7.4 (Figure 2d, inset).

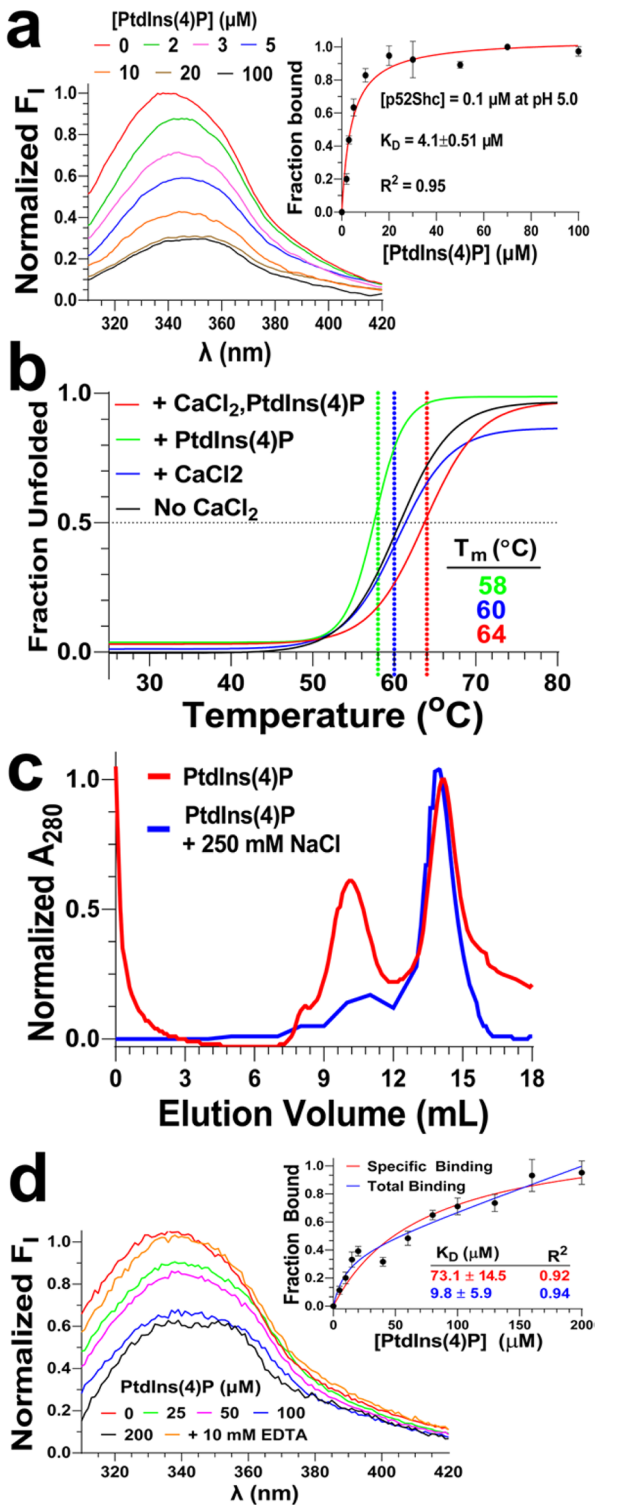

Figure 2. Spectroscopic studies of the interaction between p52Shc and PtdIns(4)P. (a) PtdIns(4)P titration at pH 5.0 and 25 °C monitored by fluorescence spectroscopy. The tryptophan fluorescence of p52Shc was recorded using a λ_{ex} of 295 nm at the indicated PtdIns(4)P concentration. The normalized fluorescence intensity was plotted vs the emission wavelength. PtdIns(4)P binding data at pH 5.0 (inset) were fit to a 1:1 binding model as described in Experimental Procedures. The apparent dissociation constant, K_D, is indicated in the figure. (b) Thermal unfolding of p52Shc monitored by CD spectroscopy. The signal at 222 nm was monitored under different conditions. The T_m under each condition is indicated with dotted lines. (c) Size exclusion chromatogram of p52Shc at pH 7.4 in 30 μM

DOI: 10.1021/acs.biochem.5b00122
Biochemistry 2015, 54, 3469−3482

Figure 2. continued

PtdIns(4)P in the absence (red) or presence (blue) of 250 mM NaCl. (d) PtdIns(4)P titration at pH 7.4 in the presence of 100 μM $CaCl_2$. The tryptophan fluorescence of p52Shc was monitored at different concentrations of PtdIns(4)P in the presence of $CaCl_2$ at pH 7.4 and 25 °C. After p52Shc tryptophan fluorescence containing 200 μM PtdIns(4)P and 100 μM $CaCl_2$ was measured, EDTA was added to a final concentration of 10 mM, and the tryptophan fluorescence was recorded again (orange). The binding data in the presence of 100 μM $CaCl_2$ were plotted vs PtdIns(4)P concentration (inset). The data that were fit using the total (specific + nonspecific, blue) and the specific binding model (red) are shown, with the apparent K_D for each model indicated. The total and specific binding models yielded apparent K_D values of 9.8 and 73.1 μM, respectively.

When the same data were fitted to a 1:1 specific binding model, the obtained K_D [73 μM (Figure 2d, inset)] was comparable to the previously reported value of 52 μM using the isolated PTB domain.[12] To investigate the role of $CaCl_2$ in the interaction between p52Shc and PtdIns(4)P, isothermal titration calorimetry and CD spectroscopy experiments were performed. Although p52Shc did not bind to $CaCl_2$ in the absence of PtdIns(4)P (Figure S2 of the Supporting Information), the presence of both $CaCl_2$ and PtdIns(4)P shifted the midpoint of thermal unfolding by 4 °C (Figure 2b, red line). These observations indicate that $CaCl_2$ is a mediator of specific p52Shc and PtdIns(4)P interaction.

Purified Human c-Src Undergoes Autophosphorylation at Tyr419 and Binds to PtdIns(4)P at pH 7.4 in a $CaCl_2$-Independent Manner. p52Shc is known to interact with a variety of kinase binding partners, including c-Src, a key regulatory kinase that mediates a wide range of cell signaling cascades.[1,34] A previous SPR experiment showed binding of GST-mouse p52Shc fusion protein to a 19-residue c-Src peptide, derived from the kinase domain, in a phosphorylation-independent manner (K_D = 18 nM).[1] Because PtdIns(4)P binds to both p52Shc and the isolated SH3 domain of c-Src,[12,35] the lipid-mediated interaction between the two proteins may affect overall kinase reaction efficiency and determine which sites on p52Shc are phosphorylated in

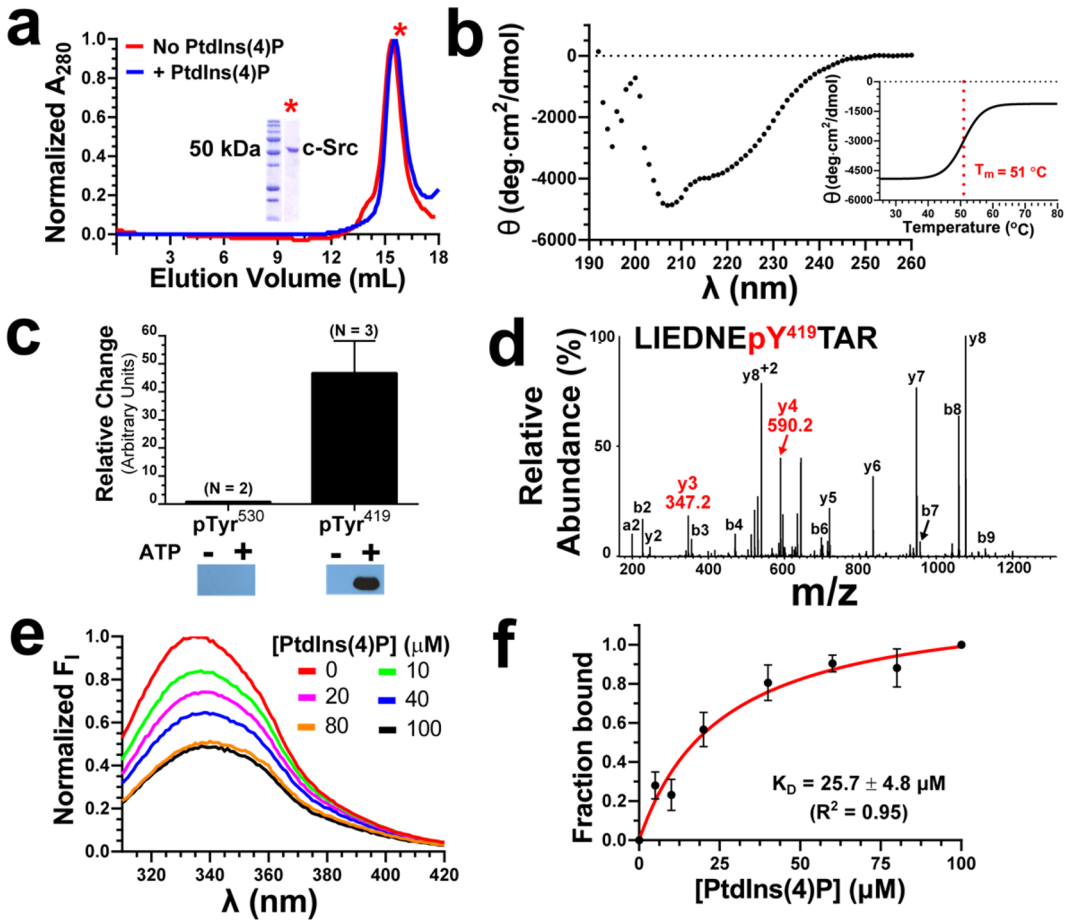

Figure 3. Purified human c-Src spanning residues 86−536 undergoes autophosphorylation at Tyr^{419} and binds to PtdIns(4)P at pH 7.4. (a) Size exclusion chromatogram of 51 kDa human c-Src, spanning residues 86−536 containing the SH3, SH2, and kinase domains. The protein eluted at an elution volume of 15.7 mL in the absence of PtdIns(4)P (red). No change in the elution volume was observed in the presence of 30 μM PtdIns(4)P (blue). (b) Far-UV CD spectrum of purified c-Src at pH 7.4 and 25 °C. The thermal unfolding of c-Src was monitored at 222 nm (inset), showing a T_m of 51 °C. (c) Western blot and densitometry analysis of c-Src autophosphorylation at Tyr^{419} or Tyr^{530} in the presence or absence of ATP. The blot was probed with the anti-pTyr419 or anti-pTyr530 c-Src antibody as indicated in the figure. The data were normalized for the reaction without ATP. (d) MS/MS spectrum of phosphorylated c-Src derived from residues 413−422 (LIEDNEY^{419}TAR) containing autophosphorylation site Y419. (e) Titration of PtdIns(4)P at pH 7.4 monitored by fluorescence spectroscopy. Tryptophan fluorescence spectra of c-Src at different PtdIns(4)P concentrations are shown as different color lines. (f) Fitting of the binding data using a 1:1 binding model yielded a K_D of 25.7 μM at pH 7.4 and 25 °C.

DOI: 10.1021/acs.biochem.5b00122
Biochemistry 2015, 54, 3469−3482

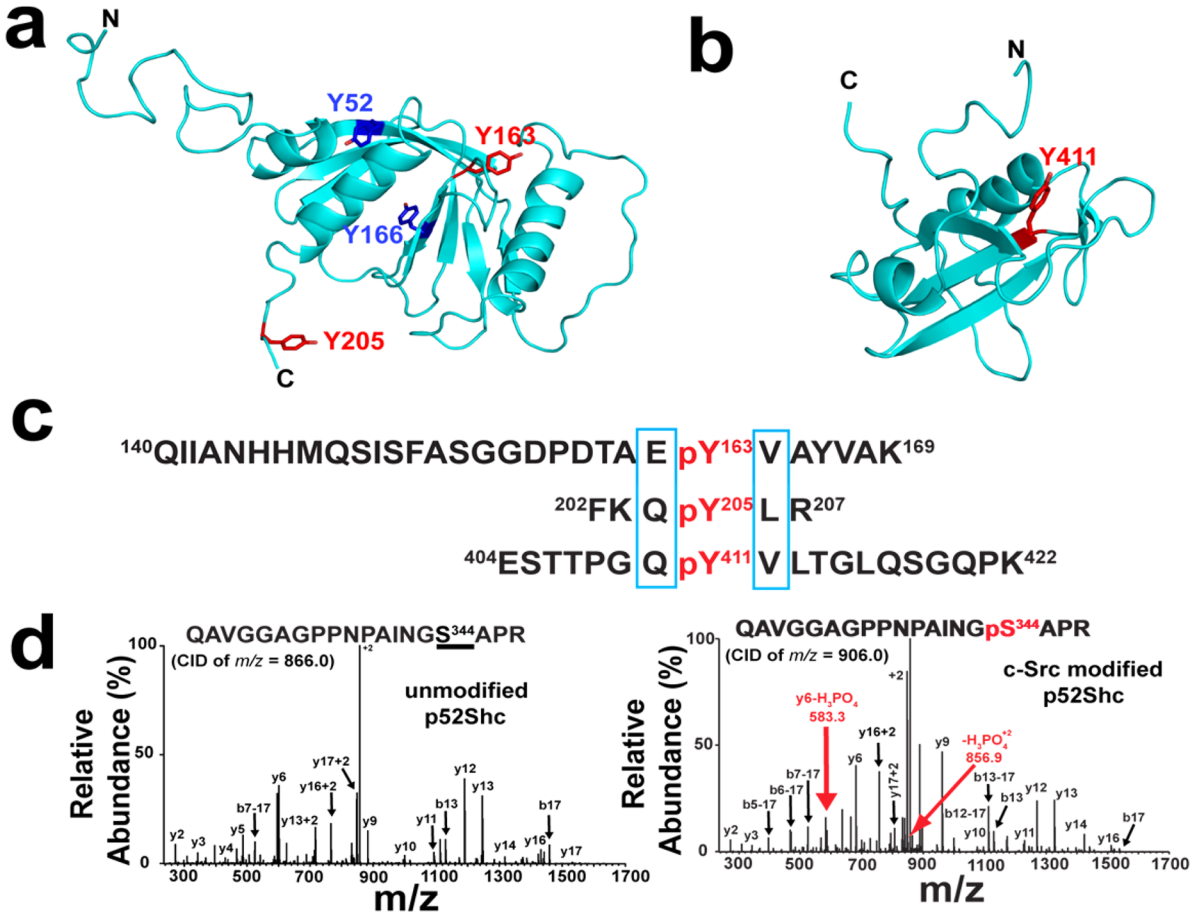

Figure 4. Cancer-associated tyrosine phosphorylation by c-Src contains the unique consensus sequence E/Q-pTyr-V/L. (a) NMR structure of the isolated PTD domain [Protein Data Bank (PDB) entry 1SHC].[12] The N-terminus and the C-terminus are labeled as N and C, respectively. Tyr163 and Tyr205 phosphorylation sites are shown as red sticks. Tyr52 and Tyr166 (blue sticks) satisfy the unique consensus sequence requirement but were not phosphorylated by c-Src. (b) Crystal structure of the isolated SH2 domain (PDB entry 1MIL)[36] with the N- and C-termini labeled. The Tyr411 phosphorylation site is shown as red sticks. (c) Amino acid sequence of the p52Shc phosphopeptide. The phosphorylation site in each peptide is colored red. Blue boxes indicate consensus phosphorylation sequences identified in this study. (d) MS/MS spectra of a peptide derived from residues 329−347 containing the Ser344 phosphorylation site. The left panel is the MS/MS spectrum of the doubly charged unmodified peptide (CID of m/z 866.0). The average of six spectra is shown. The right panel is the MS/MS spectrum of the Ser344-phosphorylated peptide (CID of m/z 906.0). Neutral loss peaks are colored red. The average of four spectra is shown.

response to c-Src activation. To test this hypothesis, human c-Src, containing SH3, SH2, and kinase domains (residues 86−536), was expressed in *E. coli* and purified to homogeneity as judged by SDS−PAGE (Figure 3a, inset). SEC and the CD spectrum of the purified protein showed that it is monomeric in solution (Figure 3a, red line) with clear secondary structure elements (Figure 3b) that undergo cooperative thermal unfolding with a T_m of 51 °C (Figure 3b and inset). Furthermore, activating autophosphorylation at Tyr419 was observed upon incubation with $MgCl_2$ and ATP (Figure 3c,d), while the inhibitory phosphorylation at Tyr530 was absent (Figure 3c). Unlike that of p52Shc, binding of c-Src to PtdIns(4)P at pH 7.4 did not require $CaCl_2$, yielding a K_D value of 25.7 μM when tryptophan fluorescence was monitored upon PtdIns(4)P titration (Figure 3e,f). In contrast to p52Shc, addition of PtdIns(4)P to c-Src did not shift the SEC elution volume (Figure 3a, blue line), which suggests that purified c-Src binds to smaller PtdIns(4)P species or, possibly, monomeric PtdIns(4)P. These results demonstrate that the human c-Src expressed in *E. coli* and purified in this study is folded and fully functional.

p52Shc Phosphorylation Does Not Require Stable Binding to c-Src. To test whether p52Shc phosphorylation by c-Src requires the formation of a stable complex, both unphosphorylated p52Shc and c-Src (200 μg each) were co-incubated for 30 min at pH 7.4 and 25 °C and subjected to SEC analysis. The total protein concentration in each elution fraction was determined by a BCA assay, and an equal amount of protein from each fraction was subjected to phosphorylation by addition of $MgCl_2$ and ATP. The kinase reaction samples were loaded onto an SDS−PAGE gel and analyzed by Western blotting using the anti-phosphotyrosine antibody for detection of both p52Shc and c-Src phosphorylation. In contrast to the previous SPR study,[1] a stable p52Shc−cSrc complex with an expected molecular mass of 103 kDa was not observed: there was no appreciable change in the SEC elution volume of p52Shc or c-Src (Figure S3 of the Supporting Information, blue line). Human c-Src eluted across both peaks 1 and 2 as evidenced by the presence of phosphorylation in both peak fractions, with a majority of p52Shc and c-Src eluting in peaks 1 and 2, respectively (Figure S3a of the Supporting Information, blue line, and Figure S3b of the Supporting Information). To test if PtdIns(4)P is required to stabilize a p52Shc−cSrc

DOI: 10.1021/acs.biochem.5b00122
Biochemistry 2015, 54, 3469−3482

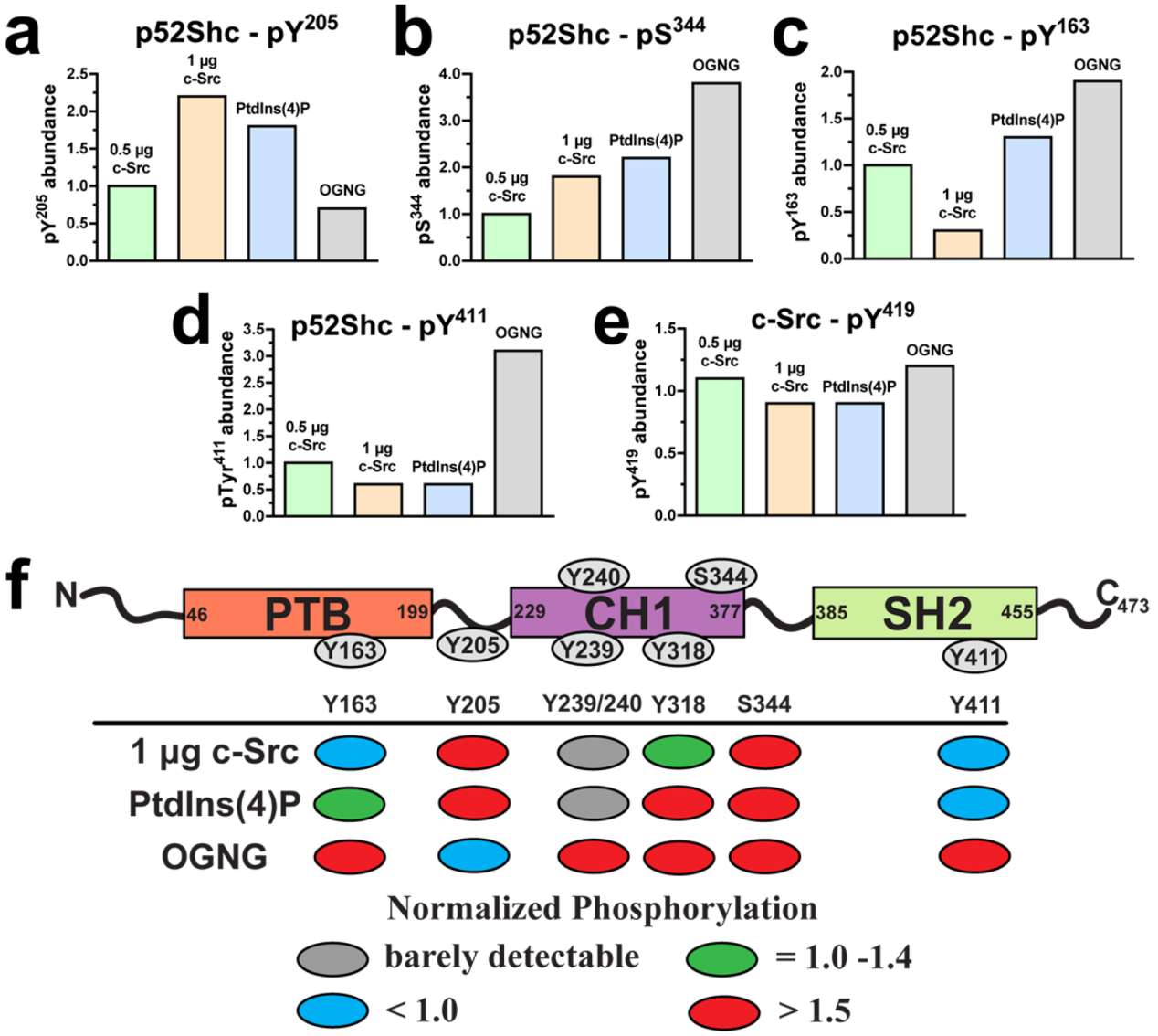

Figure 5. p52Shc phosphorylation is affected by the solution environment. (a–e) The level of phosphorylation in each peptide was quantified by the native peptide reference method as described in Experimental Procedures. The ratio of the chromatographic area for each phosphorylated and unmodified peptide (HPO_3/unmodified) was evaluated. The HPO_3/unmodified ratio for each condition was normalized to that of the corresponding 0.5 μg c-Src reaction. The normalized phosphorylation level for each peptide under different conditions is shown with bars. The phosphorylation levels are for reactions with 0.5 μg of c-Src (green), 1 μg of c-Src (blue), 0.5 μg of c-Src with 30 μM PtdIns(4)P (blue), and 0.5 μg of c-Src with 2 mM OGNG (gray). (f) p52Shc phosphorylation map. The normalized phosphorylation level for each peptide was color-coded to aid visualization. Different colors at each phosphorylation site were assigned on the basis of the normalized phosphorylation level: the normalized phosphorylation level (HPO_3/unmodified) of >1.5 (red), <1.0 (blue), 1.0–1.4 (green), and barely detectable (gray). Reaction conditions are labeled as 1 μg c-Src, PtdIns(4)P, and OGNPG. Because the level of phosphorylation at Tyr239/240 was barely detectable for the 0.5 μg c-Src reaction, the ratio (HPO_3/unmodified) derived from a Tyr163-containing peptide was used as a native reference peptide to normalize the level of phosphorylation at Tyr239/240. The Tyr163-containing peptide satisfied criteria as a native reference peptide, including similar elution time and mass spectrometry responses.

complex, both proteins were co-incubated in the presence of PtdIns(4)P prior to SEC analysis and subsequent kinase reaction. The presence of both p52Shc and a trace amount of c-Src in high-molecular mass species (denoted with an asterisk in Figure S3 of the Supporting Information) is indicated by the presence of tyrosine phosphorylation on a Western blot (Figure S3b of the Supporting Information, asterisk). However, a large majority of c-Src eluted as monomer and underwent autophosphorylation when it was co-incubated with p52Shc and PtdIns(4)P (Figure S3a of the Supporting Information, peak 2 on the red line, and Figure S3b of the Supporting Information). These results indicate that phosphorylation of p52Shc does not require the formation of a stable complex with c-Src.

Cancer-Associated p52Shc after *in Vitro* Phosphorylation by c-Src Contains Accessible E/Q-pTyr-V/L. To identify p52Shc phosphorylation sites by c-Src, kinase reactions were conducted using the purified proteins at pH 7.4 for mass spectrometry analysis combined with in-gel trypsin digestion. The peptide coverage of p52Shc in all kinase reactions tested in this study ranged from 92 to 96%, covering all tyrosine residues. Of 10 tyrosine residues in p52Shc, Tyr163 in the PTB domain, Tyr205 in a loop connecting the PTB and CH1 domains, and Tyr411 in the SH2 domain were phosphorylated. In NMR and

DOI: 10.1021/acs.biochem.5b00122
Biochemistry 2015, 54, 3469–3482

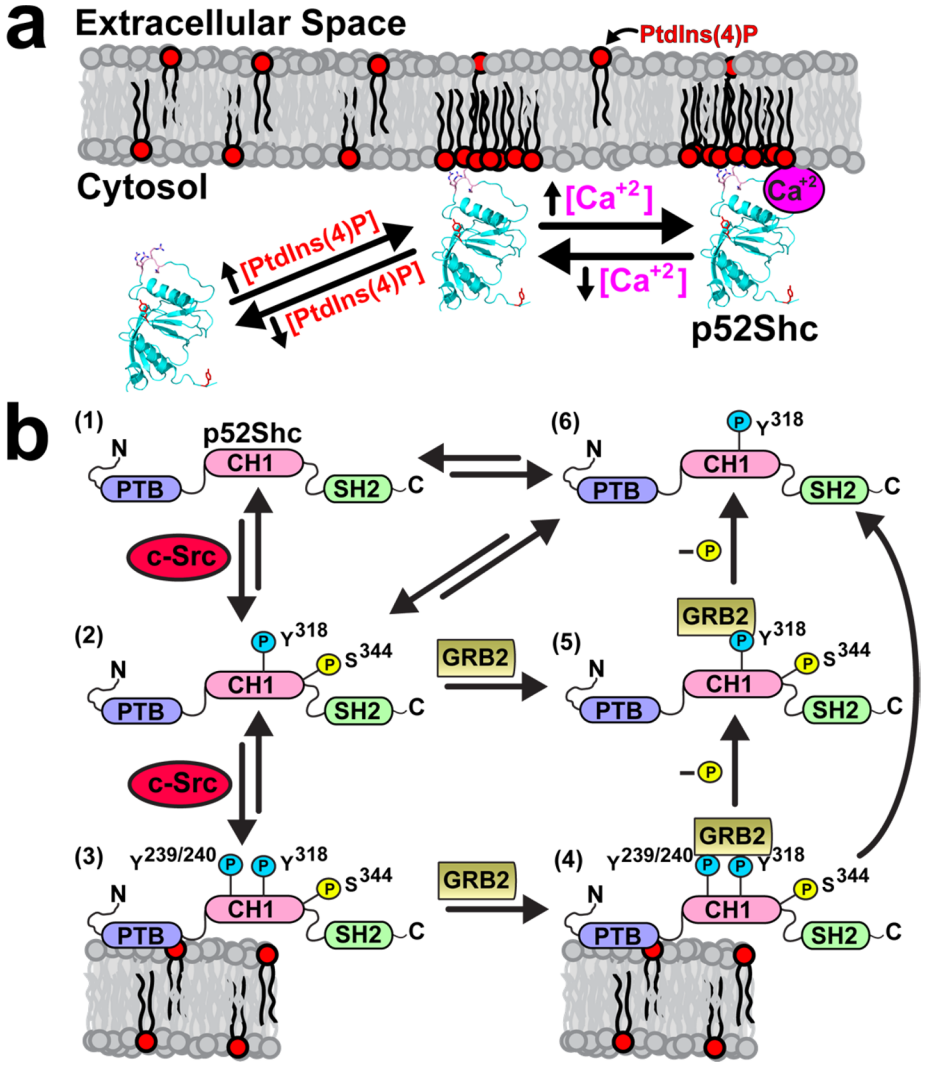

Figure 6. Human p52Shc partitions between the cytosol and the membrane surface. (a) Proposed model for the role of PtdIns(4)P and $CaCl_2$ binding in p52Shc localization. Full-length p52Shc is shown as a ribbon cartoon (represented by only the PTB domain structure; the orientation of the PTB domain is arbitrary). In the absence or low localized concentrations of PtdIns(4)P, p52Shc stays predominantly in the cytosol (left). An increased PtdIns(4)P membrane concentration facilitates the formation of PtdIns(4)P clusters and targets p52Shc to the membrane surface by nonspecific electrostatic interactions (middle). When p52Shc is at the membrane surface, the p52Shc population containing phosphorylated Tyr 239/240 and Tyr318 increases, resulting in the recruitment of Grb2 preferentially at the membrane surface. This PtdIns(4)P−p52Shc binding interaction is further facilitated by localized increases in Ca^{2+} concentration resulting in a tighter anchoring of p52Shc to the luminal face of the membrane surface that may play a role in stabilization of signaling complexes. (b) Proposed model for the interaction between p52Shc and Grb2. In the cytosol, unphosphorylated (1) or phosphorylated p52Shc at Y318 (6) and/or Ser344 (2) equilibrates. At the membrane surface, p52Shc phosphorylation at Y239/240 is favored (3), and p52Shc binds to Grb2 more tightly at the membrane surface (4). When p52Shc is away from the membrane surface, the level of phosphorylation at Y239/240 is diminished while Y318 and S344 phosphorylation is preserved (5). Alternatively, phosphatases may dephosphorylate Ser344, leading to dissociation of Grb2 (4 → 6).

crystal structures of the isolated PTB and SH2 domains,[12,36] these tyrosine residues are located in loop regions (Figure 4a,b). The sequence of these peptides is quite dissimilar to the known c-Src consensus phosphorylation sequence, E-E-I-pY-E/G-X-F, identified in a previous peptide library study.[37] Instead, the amino acid sequence of these tyrosine-phosphorylated peptides contained the following unique consensus sequence: hydrophilic (E/Q)-pTyr-large hydrophobic (L/V) (Figure 4c). However, two other tyrosine phosphorylation sites identified in this study slightly deviated from this sequence pattern. These phosphorylation sites include Tyr239/240 (Q-pTyr-N) and Tyr318 (S-pTyr-V). In addition to this consensus sequence requirement, phosphorylation sites must be accessible to the c-Src active site. This is implied by the absence of phosphorylation at Tyr52 and Tyr166 in the PTB domain. While these two tyrosine residues satisfy the consensus sequence requirement (S-Y52-L and A-Y166-V), both residues are located in the central β-sheet core region (Figure 4a). Furthermore, the lack of phosphatases and other competing kinases afforded to *in vitro* kinase reactions with the purified proteins helped us to uncover another intriguing site of phosphorylation in human p52Shc by c-Src. Although c-Src is classified as a nonreceptor tyrosine kinase, MS/MS spectra of a peptide derived from residues 339−347 showed an increase in average peptide molecular mass of 80 Da, corresponding to HPO_3, as well as H_3PO_4 neutral loss peaks (Figure 4d), unambiguously assigning the spectra to a serine phosphorylation-containing peptide. Although some kinases, including c-

DOI: 10.1021/acs.biochem.5b00122
Biochemistry 2015, 54, 3469−3482

Src, are known to be promiscuous,[2] phosphorylation of Ser344 of 30 serine residues in p52Shc implies involvement of a phosphorylation specificity mechanism more complex than the canonical sequence-based recognition mechanism. Although other cellular components may play a role in determining specific phosphorylation sites, all phosphorylation sites including Ser344 identified in this study except one (pTyr163) were previously identified in a variety of cancer tissue samples, including leukemia and breast and lung cancer, according to PhosphoSitePlus.[38]

p52Shc Conformation- and Stability-Dependent Phosphorylation. Increased intracellular concentrations of activated c-Src are associated with a variety of human cancers as well as diabetic nephropathy.[39,40] Under such pathological conditions, an increase in the amount of phosphorylated proteins by highly activated c-Src could result in prolonged activation of downstream signaling cascades. This assumes that kinase reactions involve distributive phosphorylation mechanisms in which the amount of phosphorylated proteins is proportional to the amount of activated kinases. To investigate whether phosphorylation of p52Shc by c-Src involves a distributive mechanism, the amount of c-Src in the kinase reaction was doubled to 1 μg, and the level of phosphorylation at each site was quantified by the native reference peptide method described previously.[23,24,38] In this method, mass spectrometry analysis is conducted in selected ion monitoring mode, and the chromatographic area of each unmodified and modified form for the same peptides is evaluated to obtain the ratio of phosphorylated to unphosphorylated peptide (HPO_3/unmodified). The ratio, HPO_3/unmodified, for each reaction condition was then normalized to that of a 0.5 μg c-Src reaction for the same peptide and denoted as pY or pS abundance (Figure 5a–e). Overall, the phosphorylation level at each site was site-dependent. For example, as expected for the distributive mechanism, the phosphorylation level at Tyr205 and Ser344 in the 1 μg c-Src reaction was doubled compared to that of the corresponding 0.5 μg c-Src reaction (Figure 5a,b). In contrast, the level of phosphorylation at Tyr163 and Tyr411 was reduced (Figure 5c,d), demonstrating that phosphorylation at one site affects phosphorylation at other sites. We further addressed a question of whether p52Shc conformation influences the pattern or amount of phosphorylated p52Shc. Because the addition of PtdIns(4)P influenced the biophysical properties of p52Shc (Figure 2), a kinase reaction was conducted in the presence of PtdIns(4)P using 0.5 μg of c-Src, and the phosphorylation level of each peptide was quantified. The results are mapped onto the p52Shc domain structure (Figure 5f) to identify possible functional relationships among the phosphorylation sites. Interestingly, in the presence of PtdIns(4)P, altered phosphorylation levels were observed without changing the overall phosphorylation pattern. For instance, Tyr163 phosphorylation was enhanced more than that of the 1 μg c-Src reaction (Figure 5c,f). An increased level of Tyr163 phosphorylation in the PTB domain coincided with the increased level of phosphorylation at Tyr318 in the CH1 domain (Figure 5f). More importantly, these changes in the phosphorylation level were not due to an increase in the active fraction of c-Src because the percentage ratio of unphosphorylated and phosphorylated c-Src at Tyr419, the activating autophosphorylation site, was always close to 50% under all conditions investigated in this study (Figure 5e). Therefore, the observed changes in the phosphorylation level should solely depend on p52Shc conformation and stability. Because phosphorylated p52Shc mediates assembly of signaling complexes at the membrane surface, including insulin receptor signaling,[5] kinase reactions were also conducted in a membrane-mimetic environment using the amphiphilic OGNG detergent that has an uncharged hydrophilic headgroup. OGNG is a member of the maltose-neopentyl glycol family of amphiphilic detergents designed to facilitate solubilization and stabilization of polytopic integral membrane proteins.[41] Under our experimental conditions, where OGNG exists predominantly in micellar form, distinct phosphorylation levels were again observed. For example, a reduced level of Tyr205 phosphorylation correlated with an increased level of phosphorylation at Tyr411 (Figure 5f), suggestive of an antagonistic functional role between these two sites. This reduction in the phosphorylation abundance at Tyr411 could be due to Tyr205 phosphorylation- or OGNG-induced p52Shc conformational changes that block access to Tyr411 by c-Src. Intriguingly, the Grb2 binding site, composed of Tyr239, Tyr240, and Tyr318 in the CH1 domain, was robustly phosphorylated upon addition of OGNG (Figures 5f and 6b), as evidenced by an 80 Da (-HPO_3) increase in the average molecular mass of the phosphopeptide compared to that of the unmodified peptide (Figure S4a,b of the Supporting Information). This observation suggests that the membrane surface primes the p52Shc conformation for these tyrosine phosphorylation events and subsequent Grb2 binding. This increased level of phosphorylation at the Grb2 binding site was also correlated with the thermal stability of p52Shc: in the presence of OGNG, p52Shc was the least stable (Figure S5 of the Supporting Information; T_m = 55 °C), implying that tyrosine phosphorylation at positions 239, 240, and 318 involves partial unfolding of p52Shc. These findings suggest that partitioning of p52Shc between the cytosol and the membrane surface impacts p52Shc phosphorylation abundance. This is likely to be important in selecting p52Shc binding partners and, as a result, in determining which downstream signaling cascades are activated.

DISCUSSION

Adaptor proteins are traditionally viewed as passive mediators in the activation of signaling cascades by serving as molecular platforms.[42] In this classical view of signal activation, p52Shc phosphorylation is a key determinant in selecting its binding partner among numerous others followed by migration of a bound complex to the membrane surface where it interacts with receptor tyrosine kinases.[5] On the other hand, the protein landscape model envisions the ensemble of preexisting conformers and the population redistribution within this ensemble after changes in the surrounding environment or ligand binding have taken place.[43] This implies that p52Shc prepartitioning between the cytosol and the membrane surface, prior to its phosphorylation, could determine the phosphorylation site as well as abundance by priming p52Shc conformation and stability. To test this hypothesis, we first characterized purified p52Shc and its binding partner, c-Src, in aqueous and membrane-mimetic environments using biochemical and biophysical methods (Figures 1–3). Despite its multimodular architecture, p52Shc underwent cooperative two-state thermal unfolding (Figure 2b), suggesting that the entire protein consists of one cooperative unit. This property is likely to be important in facilitating domain–domain communication in p52Shc following changes in local environment or side chain modification (e.g., phosphorylation). On the

DOI: 10.1021/acs.biochem.5b00122
Biochemistry 2015, 54, 3469–3482

basis of a previous study using the isolated PTB domain,[12] we characterized the full-length human p52Shc conformation and stability in the presence of PtdIns(4)P, a negatively charged lipid in the inner leaflet of the plasma membrane.[44] Under our experimental conditions, PtdIns(4)P formed clusters (Figure S1 of the Supporting Information) that mimic a raftlike environment.[29−32] We demonstrate that the interaction between PtdIns(4)P and p52Shc is destabilizing (Figure 2b; T_m = 58 °C) and induces partitioning of p52Shc between the monomer and PtdIns(4)P cluster−p52Shc complex (Figure 2c). The binding of PtdIns(4)P to p52Shc at pH 7.4 was readily dispersed by addition of NaCl (Figure 2c), indicating that the binding is reversible and mediated via electrostatic interactions. As observed in other proteins containing lipid binding modules such as C2, FERM, and MARCKS,[45] the interaction between p52Shc and PtdIns(4) was nonspecific at pH 7.4. These findings suggest that the nonspecific interaction of p52Shc with PtdIns(4)P is likely to play a role in p52Shc membrane targeting as well as bifurcation of activated signaling cascades to the cytosolic and receptor-mediated signaling pathways. This is implied by the p52Shc partitioning (Figure 2c) as well as the distinct phosphorylation level observed in the presence of PtdIns(4)P (Figure 5). In particular, a prominent increase in the level of Tyr318 phosphorylation, one of the key phosphorylation sites for Grb2 binding,[9,46] suggests preferential recruitment of Grb2 at the raftlike membrane surface rather than away from the membrane in the cytosol. More importantly, changes in p52Shc phosphorylation level are associated with p52Shc stability without affecting the fraction of active c-Src, demonstrating p52Shc conformation-dependent phosphorylation. We also found that $CaCl_2$ mediates specific interaction between p52Shc and PtdIns(4)P (Figure 2d), which results in the stabilization of p52Shc as evidenced by the increased midpoint of thermal denaturation (Figure 2b). On the basis of these observations, the following PtdIns(4)P-mediated p52Shc localization model is proposed (Figure 6a). In the absence of PtdIns(4)P, monomeric p52Shc predominantly exists in the cytosol. An increase in the PtdIns(4)P concentration facilitates formation of the acidic lipid-rich clusters in membranes that function to target p52Shc to these clusters via nonspecific electrostatic interactions. This p52Shc partitioning prior to its phosphorylation not only determines the site and abundance of phosphorylation but also aids in the selection of the resultant binding partner. An increase in the intracellular Ca^{2+} concentration, as observed in EGF-stimulated cells,[47] mediates specific binding between p52Shc and PtdIns(4)P by serving as an interaction bridge, resulting in anchoring of p52Shc at specific membrane sites. This Ca^{2+}-mediated stable interaction between p52Shc and PtdIns(4)P could also play a role in determining the duration of signal propagation by stabilizing a signaling complex being assembled at the membrane surface. This model may also be important in p52Shc-mediated EGFR transfer between endosomes and lysosomes during receptor degradation as PtdIns(4)P is known to accumulate in these acidic compartments.[28,48] This is supported by the increased PtdIns(4)P binding affinity at acidic pH (Figure 2a), implying that p52Shc may have an additional role in EGFR receptor trafficking from the plasma membrane to these acidic organelles.

To further study how the chemical property of lipid impacts p52Shc phosphorylation, we used an uncharged nonionic detergent (OGNG) to mimic a membrane environment. A correlation between p52Shc thermal stability and phosphorylation of the Grb2 binding region was again observed (Figure 5f). In OGNG, human p52Shc was the least stable among the conditions tested in this study (Figure S5 of the Supporting Information). When kinase reactions were conducted in the presence of OGNG, all Grb2 binding residues, including Tyr239 or Tyr240, and Tyr318 in the CH1 domain were robustly phosphorylated by c-Src, implying that the extent of p52Shc partial unfolding at the membrane surface determines the abundance of phosphorylation at Grb2 binding tyrosine residues. A previous immunoprecipitation and mutagenesis study showed that Grb2 bound to the doubly phosphorylated p52Shc peptide at Tyr239 and Tyr240 tighter than the singly phosphorylated p52Shc peptide at Tyr318.[9] Together with our experimental observations, it is likely that the composition and chemical properties of lipids in the membrane determine the extent of p52Shc partial unfolding at the membranes surface, and that dictates the level of subsequent phosphorylation in the Grb2 binding region in the CH2 domain. This further suggests that the biophysical properties of p52Shc play an important role in regulating signaling cascade activation.

This study also demonstrates that c-Src phosphorylates Ser344 of p52Shc despite being classified as a nonreceptor tyrosine kinase. While this may indicate the promiscuous nature of c-Src activity, the selection of this specific serine residue out of 30 serine residues in p52Shc argues against nonspecific or adventitious phosphorylation. Indeed, a similar observation was made in a previous study using affinity-purified p52Shc expressed in mouse embryonic fibroblasts.[6] In this previous study, when murine p52Shc was phosphorylated by c-Src, Erk1, or AKT1, Ser355 (corresponding to Ser344 in human p52Shc) phosphorylation was consistently observed. This suggests that phosphorylation specificity may not be solely determined by the identity of kinases, and it further indicates the importance of the conformation and/or stability of kinase substrates in determining downstream phosphorylation events. The importance of this Ser phosphorylation was highlighted in this same previous study where a mutation to alanine at Ser355 in mouse p52Shc caused a loss of binding to a majority of p52Shc binding partners, including Grb2,[6] suggesting that phosphorylation at this site is crucial for stabilizing signaling complexes. These data support the following model for the interaction of p52Shc with Grb2 (Figure 6b). Unphosphorylated [labeled (1)] and phosphorylated [labeled (2) and (6)] p52Shc at Y318 and/or S344 equilibrate in the cytoplasm. Singly phosphorylated p52Shc at Y318 binds weakly to Grb2 in the cytosol [labeled (5) in Figure 6b]. Upon p52Shc localization at the membrane surface, Y239/240 is heavily phosphorylated (Figure 5f), resulting in the recruitment of Grb2 [labeled (4) in Figure 6b]. In the cytosol, Y239/240 phosphorylation is poorly retained, resulting in weaker Grb2 binding or complete dissociation from p52Shc. Although stepwise dephosphorylation at Y239/240 and Y318 also can cause Grb2 dephosphorylation, these steps may be bypassed by dephosphorylation at Ser344, resulting in Grb2 dissociation [(5) to (6) in Figure 6b]. Alternatively, multiple tyrosine phosphorylation events and serine phosphorylation by c-Src may indicate the importance of kinetic proofreading as an error-reduction mechanism whereby the level of nonspecific, or "off-target", phosphorylation is reduced via the coupled action of phosphatases.[2,49] This is important in activating desirable signaling cascades in an environment-dependent manner, and it is intriguing that the additional p52Shc phosphorylation sites observed in this study are also found in human cancers.[38] In addition to these cancer-

DOI: 10.1021/acs.biochem.5b00122
Biochemistry 2015, 54, 3469−3482

associated p52Shc phosphorylation sites, we discovered a novel site of tyrosine phosphorylation by c-Src at Tyr163 of p52Shc. This phosphorylation is likely to be transient phosphorylation *in vivo* as previous p52Shc phosphorylation studies using classical pull-down assays and Western blots were unable to detect phosphorylation at Tyr163. Transient phosphorylation may be important in the rapid assembly and/or disassembly of signaling complexes, while stable phosphorylation serves as a molecular platform for protein docking and binding events. Interestingly, Tyr163 appears to be the most sensitive to changes in environment (Figure 5f) as seen in the variable phosphorylation abundance under each experimental condition. The *in vivo* expression of p52Shc carrying a mutation at transient phosphorylation sites will be necessary to study the role of transient phosphorylation in biological signal propagation and disease progression.

In the classical view of signaling activation mechanisms, kinases play the central role in regulating signaling cascades via phosphorylation.[2] For that reason, they have been considered as major therapeutic targets.[50] This study suggests that p52Shc conformational stability and membrane binding influence phosphorylation site specificity and abundance. These properties may be exploited to alter the activation or duration of biological signaling cascades for therapeutic purposes. For example, to block prolonged activation of Ras/MAPK/ERK signaling by preventing p52Shc and Grb2 interaction, the combined action of phosphatases and shifting the conformational equilibrium of p52Shc to the cytosolic form could serve as an effective strategy for suppressing Tyr239/240 phosphorylation.

■ ASSOCIATED CONTENT

Supporting Information

Dynamic light scattering of PtdIns(4)P at pH 5.0 and 7.4 (Figure S1), isothermal titration calorimetry of p52Shc titrated with $CaCl_2$ (Figure S2), an illustration of the absence of p52Shc and c-Src complex formation with or without PtdIns(4)P (Figure S3), far-UV CD spectrum of p52Shc and the thermal denaturation experiments in the presence of detergent OGNG (Figure S4), and MS/MS spectra of p52Shc phosphopeptides containing Tyr318 and Tyr239/240 (Figure S5). The Supporting Information is available free of charge on the ACS Publications website at DOI: 10.1021/acs.biochem.5b00122.

■ AUTHOR INFORMATION

Corresponding Author

*E-mail: franklin-hays@ouhsc.edu. Telephone: (405) 271-2227, ext. 61213. Fax: (405) 271-3092.

Funding

Research reported in this study was supported by an Institutional Development Award (IDeA) from the National Institute of General Medical Sciences of the National Institutes of Health via Grant P20GM104934 and National Science Foundation Grant NSF-ACI-1339649 (to B.D.). Supercomputer time allocations were provided through National Science Foundation Grant TG-MCB070039 (to B.D.). We acknowledge the support of San Antonio Cancer Institute Grant P30 CA054174 for the Center for Analytical Ultracentrifugation of Macromolecular Assemblies at the University of Texas Health Science Center at San Antonio and the Oklahoma Medical Research Foundation for support of the mass spectrometry facility used for this study.

Notes

The authors declare no competing financial interest.

■ ACKNOWLEDGMENTS

We thank Drs. Ann Louise Olson, Paul Weigel, Jian-Xing Ma, and Donald Capra at the University of Oklahoma Health Sciences Center for helpful comments and suggestions during the course of these studies and Dr. Pradman Qasba at the National Institutes of Health for providing the pLgals1 plasmid.

■ ABBREVIATIONS

EGF, epidermal growth factor; 2DSA, two-dimensional spectrum analysis; AUC, analytical ultracentrifugation; BCA, bicinchoninic acid; BrPC, 1,2-distearoyl(dibromo)-*sn*-glycero-3-phosphocholine; DLS, dynamic light scattering; FAK, focal adhesion kinase; FERM, 4.1, ezrin, radixin, moesin; IPTG, isopropyl β-D-thiogalactopyranoside; MARCKS, myristoylated alanine-rich C-kinase substrate; MS/MS, product ion spectrum; OGNG, 2,2-dihexylpropane-1,3-bis-β-D-glucopyranoside; PtdIns(4)P, phosphatidylinositol 4-phosphate; SEC, size exclusion chromatography; SV, sedimentation velocity; TBST, Tris-buffered-serine-Tween-20.

■ REFERENCES

(1) Sato, K., Nagao, T., Kakumoto, M., Kimoto, M., Otsuki, T., Iwasaki, T., Tokmakov, A. A., Owada, K., and Fukami, Y. (2002) Adaptor protein Shc is an isoform-specific direct activator of the tyrosine kinase c-Src. *J. Biol. Chem. 277*, 29568−29576.

(2) Ubersax, J. A., and Ferrell, J. E., Jr. (2007) Mechanisms of specificity in protein phosphorylation. *Nat. Rev. Mol. Cell Biol. 8*, 530−541.

(3) Gehart, H., Kumpf, S., Ittner, A., and Ricci, R. (2010) MAPK signalling in cellular metabolism: Stress or wellness? *EMBO Rep. 11*, 834−840.

(4) Kim, E. K., and Choi, E. J. (2010) Pathological roles of MAPK signaling pathways in human diseases. *Biochim. Biophys. Acta 1802*, 396−405.

(5) Wills, M. K., and Jones, N. (2012) Teaching an old dogma new tricks: Twenty years of Shc adaptor signalling. *Biochem. J. 447*, 1−16.

(6) Zheng, Y., Zhang, C., Croucher, D. R., Soliman, M. A., St-Denis, N., Pasculescu, A., Taylor, L., Tate, S. A., Hardy, W. R., Colwill, K., Dai, A. Y., Bagshaw, R., Dennis, J. W., Gingras, A. C., Daly, R. J., and Pawson, T. (2013) Temporal regulation of EGF signalling networks by the scaffold protein Shc1. *Nature 499*, 166−171.

(7) McGlade, J., Cheng, A., Pelicci, G., Pelicci, P. G., and Pawson, T. (1992) Shc proteins are phosphorylated and regulated by the v-Src and v-Fps protein-tyrosine kinases. *Proc. Natl. Acad. Sci. U.S.A. 89*, 8869−8873.

(8) Rozakis-Adcock, M., McGlade, J., Mbamalu, G., Pelicci, G., Daly, R., Li, W., Batzer, A., Thomas, S., Brugge, J., Pelicci, P. G., Schlessinger, J., Pawson, T., et al. (1992) Association of the Shc and Grb2/Sem5 SH2-containing proteins is implicated in activation of the Ras pathway by tyrosine kinases. *Nature 360*, 689−692.

(9) van der Geer, P., Wiley, S., Gish, G. D., and Pawson, T. (1996) The Shc adaptor protein is highly phosphorylated at conserved, twin tyrosine residues (Y239/240) that mediate protein-protein interactions. *Curr. Biol. 6*, 1435−1444.

(10) Yasui, N., Findlay, G. M., Gish, G. D., Hsiung, M. S., Huang, J., Tucholska, M., Taylor, L., Smith, L., Boldridge, W. C., Koide, A., Pawson, T., and Koide, S. (2014) Directed network wiring identifies a key protein interaction in embryonic stem cell differentiation. *Mol. Cell 54*, 1034−1041.

(11) Sato, K., Gotoh, N., Otsuki, T., Kakumoto, M., Aoto, M., Tokmakov, A. A., Shibuya, M., and Fukami, Y. (1997) Tyrosine

DOI: 10.1021/acs.biochem.5b00122
Biochemistry 2015, 54, 3469−3482

residues 239 and 240 of Shc are phosphatidylinositol 4,5-bisphosphate-dependent phosphorylation sites by c-Src. *Biochem. Biophys. Res. Commun. 240*, 399−404.
(12) Zhou, M. M., Ravichandran, K. S., Olejniczak, E. F., Petros, A. M., Meadows, R. P., Sattler, M., Harlan, J. E., Wade, W. S., Burakoff, S. J., and Fesik, S. W. (1995) Structure and ligand recognition of the phosphotyrosine binding domain of Shc. *Nature 378*, 584−592.
(13) Pasek, M., Boeggeman, E., Ramakrishnan, B., and Qasba, P. K. (2010) Galectin-1 as a fusion partner for the production of soluble and folded human β-1,4-galactosyltransferase-T7 in *E. coli*. *Biochem. Biophys. Res. Commun. 394*, 679−684.
(14) Strausberg, R. L., Feingold, E. A., Grouse, L. H., Derge, J. G., Klausner, R. D., Collins, F. S., Wagner, L., Shenmen, C. M., Schuler, G. D., Altschul, S. F., Zeeberg, B., Buetow, K. H., Schaefer, C. F., Bhat, N. K., Hopkins, R. F., Jordan, H., Moore, T., Max, S. I., Wang, J., Hsieh, F., Diatchenko, L., Marusina, K., Farmer, A. A., Rubin, G. M., Hong, L., Stapleton, M., Soares, M. B., Bonaldo, M. F., Casavant, T. L., Scheetz, T. E., Brownstein, M. J., Usdin, T. B., Toshiyuki, S., Carninci, P., Prange, C., Raha, S. S., Loquellano, N. A., Peters, G. J., Abramson, R. D., Mullahy, S. J., Bosak, S. A., McEwan, P. J., McKernan, K. J., Malek, J. A., Gunaratne, P. H., Richards, S., Worley, K. C., Hale, S., Garcia, A. M., Gay, L. J., Hulyk, S. W., Villalon, D. K., Muzny, D. M., Sodergren, E. J., Lu, X., Gibbs, R. A., Fahey, J., Helton, E., Ketteman, M., Madan, A., Rodrigues, S., Sanchez, A., Whiting, M., Madan, A., Young, A. C., Shevchenko, Y., Bouffard, G. G., Blakesley, R. W., Touchman, J. W., Green, E. D., Dickson, M. C., Rodriguez, A. C., Grimwood, J., Schmutz, J., Myers, R. M., Butterfield, Y. S., Krzywinski, M. I., Skalska, U., Smailus, D. E., Schnerch, A., Schein, J. E., Jones, S. J., Marra, M. A., and Mammalian Gene Collection Program (2002) Generation and initial analysis of more than 15,000 full-length human and mouse cDNA sequences. *Proc. Natl. Acad. Sci. U.S.A. 99*, 16899−16903.
(15) Perry, R. D., Straley, S. C., Fetherston, J. D., Rose, D. J., Gregor, J., and Blattner, F. R. (1998) DNA sequencing and analysis of the low-Ca^{2+}-response plasmid pCD1 of *Yersinia pestis* KIM5. *Infect. Immun. 66*, 4611−4623.
(16) Seeliger, M. A., Young, M., Henderson, M. N., Pellicena, P., King, D. S., Falick, A. M., and Kuriyan, J. (2005) High yield bacterial expression of active c-Abl and c-Src tyrosine kinases. *Protein Sci. 14*, 3135−3139.
(17) Demeler, B., Gorbet, G., Zollars, D., Dubbs, B., Brookes, E., and Cao, W. (2014) *Ultrascan-III version 2.2: A comprehensive data analysis software package for analytical ultracentrifugation experiments* (http://www.ultrascan3.uthscsa.edu/).
(18) Demeler, B. (2010) Methods for the Design and Analysis of Sedimentation Velocity and Sedimentation Equilibrium Experiments with Proteins. *Current Protocols in Protein Science*, Chapter 7, Unit 7.13, Wiley, New York.
(19) Brookes, E., Cao, W., and Demeler, B. (2010) A two-dimensional spectrum analysis for sedimentation velocity experiments of mixtures with heterogeneity in molecular weight and shape. *Eur. Biophys. J. 39*, 405−414.
(20) Brookes, E. H., and Demeler, B. (2007) Parsimonious Regularization using Genetic Algorithms Applied to the Analysis of Analytical Ultracentrifugation Experiments. *Proceedings of the 9th annual conference on Genetic and evolutionary computation*, ACM, Inc.
(21) Brookes, E., and Demeler, B. (2008) Parallel computational techniques for the analysis of sedimentation velocity experiments in UltraScan. *Colloid Polym. Sci. 286*, 139−148.
(22) Demeler, B., and van Holde, K. E. (2004) Sedimentation velocity analysis of highly heterogeneous systems. *Anal. Biochem. 335*, 279−288.
(23) Ruse, C. I., Willard, B., Jin, J. P., Haas, T., Kinter, M., and Bond, M. (2002) Quantitative dynamics of site-specific protein phosphorylation determined using liquid chromatography electrospray ionization mass spectrometry. *Anal. Chem. 74*, 1658−1664.
(24) Willard, B. B., Ruse, C. I., Keightley, J. A., Bond, M., and Kinter, M. (2003) Site-specific quantitation of protein nitration using liquid chromatography/tandem mass spectrometry. *Anal. Chem. 75*, 2370−2376.
(25) Kohn, J. E., Millett, I. S., Jacob, J., Zagrovic, B., Dillon, T. M., Cingel, N., Dothager, R. S., Seifert, S., Thiyagarajan, P., Sosnick, T. R., Hasan, M. Z., Pande, V. S., Ruczinski, I., Doniach, S., and Plaxco, K. W. (2004) Random-coil behavior and the dimensions of chemically unfolded proteins. *Proc. Natl. Acad. Sci. U.S.A. 101*, 12491−12496.
(26) Wilkins, D. K., Grimshaw, S. B., Receveur, V., Dobson, C. M., Jones, J. A., and Smith, L. J. (1999) Hydrodynamic radii of native and denatured proteins measured by pulse field gradient NMR techniques. *Biochemistry 38*, 16424−16431.
(27) Uversky, V. N. (2011) Intrinsically disordered proteins from A to Z. *Int. J. Biochem. Cell Biol. 43*, 1090−1103.
(28) Authier, F., and Chauvet, G. (1999) In vitro endosome-lysosome transfer of dephosphorylated EGF receptor and Shc in rat liver. *FEBS Lett. 461*, 25−31.
(29) Redfern, D. A., and Gericke, A. (2004) Domain formation in phosphatidylinositol monophosphate/phosphatidylcholine mixed vesicles. *Biophys. J. 86*, 2980−2992.
(30) Redfern, D. A., and Gericke, A. (2005) pH-dependent domain formation in phosphatidylinositol polyphosphate/phosphatidylcholine mixed vesicles. *J. Lipid Res. 46*, 504−515.
(31) Minogue, S., Chu, K. M., Westover, E. J., Covey, D. F., Hsuan, J. J., and Waugh, M. G. (2010) Relationship between phosphatidylinositol 4-phosphate synthesis, membrane organization, and lateral diffusion of PI4KIIα at the trans-Golgi network. *J. Lipid Res. 51*, 2314−2324.
(32) van den Bogaart, G., Meyenberg, K., Risselada, H. J., Amin, H., Willig, K. I., Hubrich, B. E., Dier, M., Hell, S. W., Grubmuller, H., Diederichsen, U., and Jahn, R. (2011) Membrane protein sequestering by ionic protein-lipid interactions. *Nature 479*, 552−555.
(33) Wymann, M. P., and Schneiter, R. (2008) Lipid signalling in disease. *Nat. Rev. Mol. Cell Biol. 9*, 162−176.
(34) Sato, K., Iwasaki, T., and Fukami, Y. (2005) Association of c-Src with p52Shc in mitotic NIH3T3 cells as revealed by Src-Shc binding site-specific antibodies. *J. Biochem. 137*, 61−67.
(35) Perez, Y., Maffei, M., Igea, A., Amata, I., Gairi, M., Nebreda, A. R., Bernado, P., and Pons, M. (2013) Lipid binding by the Unique and SH3 domains of c-Src suggests a new regulatory mechanism. *Sci. Rep. 3*, 1295.
(36) Mikol, V., Baumann, G., Zurini, M. G., and Hommel, U. (1995) Crystal structure of the SH2 domain from the adaptor protein SHC: A model for peptide binding based on X-ray and NMR data. *J. Mol. Biol. 254*, 86−95.
(37) Songyang, Z., Carraway, K. L., Eck, M. J., Harrison, S. C., Feldman, R. A., Mohammadi, M., Schlessinger, J., Hubbard, S. R., Smith, D. P., Eng, C., Lorenzo, M. J., Ponder, B. A. J., Mayer, B. J., and Cantley, L. C. (1995) Catalytic Specificity of Protein-Tyrosine Kinases Is Critical for Selective Signaling. *Nature 373*, 536−539.
(38) Hornbeck, P. V., Kornhauser, J. M., Tkachev, S., Zhang, B., Skrzypek, E., Murray, B., Latham, V., and Sullivan, M. (2012) PhosphoSitePlus: A comprehensive resource for investigating the structure and function of experimentally determined post-translational modifications in man and mouse. *Nucleic Acids Res. 40*, D261−D270.
(39) Irby, R. B., and Yeatman, T. J. (2000) Role of Src expression and activation in human cancer. *Oncogene 19*, 5636−5642.
(40) Taniguchi, K., Xia, L., Goldberg, H. J., Lee, K. W., Shah, A., Stavar, L., Masson, E. A., Momen, A., Shikatani, E. A., John, R., Husain, M., and Fantus, I. G. (2013) Inhibition of Src kinase blocks high glucose-induced EGFR transactivation and collagen synthesis in mesangial cells and prevents diabetic nephropathy in mice. *Diabetes 62*, 3874−3886.
(41) Chae, P. S., Rasmussen, S. G., Rana, R. R., Gotfryd, K., Kruse, A. C., Manglik, A., Cho, K. H., Nurva, S., Gether, U., Guan, L., Loland, C. J., Byrne, B., Kobilka, B. K., and Gellman, S. H. (2012) A new class of amphiphiles bearing rigid hydrophobic groups for solubilization and stabilization of membrane proteins. *Chemistry 18*, 9485−9490.
(42) Csiszar, A. (2006) Structural and functional diversity of adaptor proteins involved in tyrosine kinase signalling. *BioEssays 28*, 465−479.

DOI: 10.1021/acs.biochem.5b00122
Biochemistry 2015, 54, 3469−3482

(43) Tsai, C. J., Ma, B., and Nussinov, R. (1999) Folding and binding cascades: Shifts in energy landscapes. *Proc. Natl. Acad. Sci. U.S.A. 96*, 9970−9972.
(44) Hammond, G. R., Fischer, M. J., Anderson, K. E., Holdich, J., Koteci, A., Balla, T., and Irvine, R. F. (2012) PI4P and PI(4,5)P2 are essential but independent lipid determinants of membrane identity. *Science 337*, 727−730.
(45) DiNitto, J. P., Cronin, T. C., and Lambright, D. G. (2003) Membrane recognition and targeting by lipid-binding domains. *Sci. Signaling 2003*, re16.
(46) Gotoh, N., Toyoda, M., and Shibuya, M. (1997) Tyrosine phosphorylation sites at amino acids 239 and 240 of Shc are involved in epidermal growth factor-induced mitogenic signaling that is distinct from Ras/mitogen-activated protein kinase activation. *Mol. Cell. Biol. 17*, 1824−1831.
(47) Kim, E. K., and Choi, E. J. (2010) Pathological roles of MAPK signaling pathways in human diseases. *Biochim. Biophys. Acta 1802*, 396−405.
(48) Hammond, G. R., Machner, M. P., and Balla, T. (2014) A novel probe for phosphatidylinositol 4-phosphate reveals multiple pools beyond the Golgi. *J. Cell Biol. 205*, 113−126.
(49) Hopfield, J. J. (1974) Kinetic proofreading: A new mechanism for reducing errors in biosynthetic processes requiring high specificity. *Proc. Natl. Acad. Sci. U.S.A. 71*, 4135−4139.
(50) Rask-Andersen, M., Zhang, J., Fabbro, D., and Schioth, H. B. (2014) Advances in kinase targeting: Current clinical use and clinical trials. *Trends Pharmacol. Sci. 35*, 604−620.

DOI: 10.1021/acs.biochem.5b00122
Biochemistry 2015, 54, 3469−3482